Published in final edited form as:
Adv Drug Deliv Rev. 2009 October 5; 61(12): 1043–1054. doi:10.1016/j.addr.2009.07.013.

Electrohydrodynamics: A facile technique to fabricate drug delivery systems

Syandan Chakraborty, **I-Chien Liao**, **Andrew Adler**, and **Kam W. Leong***
Biomedical Engineering Department, Pratt School of Engineering, Duke University, Durham, NC 27708-0281.

Abstract

Electrospinning and electrospraying are facile electrohydrodynamic fabrication methods that can generate drug delivery systems (DDS) through a one-step process. The nano-structured fiber and particle morphologies produced by these techniques offer tunable release kinetics applicable to diverse biomedical applications. Coaxial-electrospinning/electrospraying, a relatively new technique of fabricating core-shell fibers/particles have added to the versatility of these DDS by affording a near zero-order drug release kinetics, dampening of burst release, and applicability to a wider range of bioactive agents. Controllable electrospinning/spraying of fibers and particles and subsequent drug release from these chiefly polymeric vehicles depends on well-defined solution and process parameters. The additional drug delivery capability from electrospun fibers can further enhance the material's functionality in tissue engineering applications. This review discusses the state-of-the-art of using electrohydrodynamic technique to generate nano-fiber/particles as drug delivery devices.

Keywords

Electrospinning; Electrospraying; Nanofiber; Nanoparticle; Drug delivery systems; Core-shell nanofibers; Coaxial electrospinning; Controlled release; Tissue engineering

1. Introduction

Modern therapeutics emphasizes pharmacokinetic and pharmacodynamic principle-driven administration of drugs. The scope of the term 'drug' has grown over the last few decades to include growth factors, bioactive proteins, and nucleic acids. This evolution continues to fuel new development of drug delivery systems (DDS) to realize the therapeutic potential of these delicate and macromolecular bioactive agents. Different materials and formats have been developed for the delivery of these bioactive agents in various contexts. A thorough discussion of all these delivery vehicles and materials is beyond the scope of this review. However, these topics have been extensively reviewed by several authors [1–3]. One interesting development is the application of electrohydrodynamics to fabricate drug-loaded nanofibers and nanoparticles. The former responds to requirement of an optimal microenvironment for regenerative medicine, and the latter to demands of targeted and intracellular delivery.

*To whom correspondence should be addressed: Biomedical Engineering Department, Pratt School of Engineering, Duke University, 1395 CIEMAS, Durham, NC: 27708-0281, Phone: (919) 660-8466, kam.leong@duke.edu.

Electrohydrodynamics, referring to the dynamics of electrically charged fluids, constitutes the basis for electrospinning and electrospraying. In electrospinning, when electrical forces overcome the forces of surface tension in the charged polymer liquid, a charged jet ejected from the tip of a capillary tube elongates and moves towards a grounded surface. The solvent in the jet is evaporated during the flight, leading to a mat of nanofibers deposited on the surface. The fibers are continuous and can range in diameter from several nanometers to micrometers. A limited ordering of the fibers, such as alignment, can be obtained by manipulation of the collector or the electrical field. Electrospun fibers have attracted intense attention in the field of tissue engineering because of its ease of fabrication and its resemblance to nanotopographical elements in the extracellular matrix of tissues [4]. Researchers are also increasingly interested in incorporating drugs into the fibers to enhance the functionality of these scaffolding materials.

Drugs can be embedded in the fiber through dissolution or dispersion in the polymer solution. Controlled release function integrated into a tissue engineering scaffold can offer temporal-spatial gradient of biochemical signals to mimic the complex tissue microenvironment for tissue development or regeneration [5,6]. Since many interesting biochemical factors for tissue development are protein or nucleic acid in nature, they do not dissolve in organic solvent and may suffer loss of bioactivity when dispersed in the polymer solution. Co-axial electrospinning, where the drug is dissolved in an aqueous core solution and the polymer in an organic shell solution, is one approach to overcome this drawback by extruding the core and shell solutions individually through two concentric nozzles [7]. The ramifications of this promising technique will be discussed in detail in the subsequent sections.

Other techniques for nanofiber generation, which are interesting yet not widely used, are self-assembly and phase separation [8]. Self-assembly, such as that used to synthesize nanofibers from peptide amphiphiles, is attractive because of the mild condition of fabrication and the small size attainable. However, the technique is amenable only to a limited repertoire of polymers and difficult to process into a macroscopic structure. It is also challenging to obtain a sustained release kinetics from these small fibers [9]. The phase separation technique requires gelation of the polymer and extraction of solvent [10] and suffer from a lack of control over fiber arrangement. The required solvent extraction step would also prematurely leach out any drugs entrapped in the fibers.

As an off-shoot of electrospinning, electrospraying has generated immense interest as a facile method to generate micro/nano particles. Nanoparticulate drug delivery system has been the subject of intense research and expert review [11,12]. A few prominent methods of micro/nano particle formation include emulsification-evaporation [13,14], salting-out/emulsification [15, 16], nanoprecipitation [17], ionic gelation [18,19], coacervation [20], and spray-drying [21]. Emulsion-based methods have been the most extensively employed in particulate DDS fabrication [22].

It would be advantageous to synthesize nanoparticulate DDS with the following features: 1) obviation of high shearing forces (stirring or sonication); 2) high encapsulation efficiency; 3) high loading level; 4) uniform drug distribution in the matrix; 5) rid of residual surfactant; and 6) convenient and easily scalable [13,14,16,22,23]. Electrospraying and its coaxial variant are well-positioned to address these issues. Electrospraying is based on atomization of solvated polymers by electrical forces. In general, the principle of electrospraying is quite similar to that of electrospinning apart from the fact that the jet breaks down into droplets. This is usually a consequence of using a lower concentration of polymer solution than what is used in electrospinning. Drying effects along with residual charges on the particles prevent aggregate formation once they land on the target [24,25]. Spheres with a diameter of < 10 nm can be generated with this technique whereas mechanical atomizers typically produce particles with

micron dimensions. The absence of continuous high-energy shearing force is beneficial in protecting sensitive proteins or drugs.

Electrohydrodynamic techniques can in principle achieve uniform dispersion of drug within the polymeric matrix with high loading capacity and minimal drug loss. It can also be made high-throughput if multiple electrospinning/electrospraying spinnerets are used in parallel. Another advantageous aspect of this technique is that a quality check on the particles can be performed by briefly halting the process. The option of terminating the process anytime to check expenditure of often precious biopolymers and drugs is an appreciated convenience. Ease of operation and cost-effectiveness are two other benefits. The aforementioned features along with the ability to spray/spin virtually any polymer into nano-particles and fibers without altering the basic electrospraying/spinning setup has thus made electrosprayed particles and electrospun fibers attractive drug delivery vehicles.

2. Principles of electrohydrodynamic techniques

This section briefly covers the analytical and theoretical framework for modeling the processes of electrospraying and electrospinning. The scaling relations developed in the literature are useful in the context of drug delivery as they allow prediction of the effects that modulation of solution and processing parameters have on particle and fiber geometry.

Jaworek and Sobczyk provide a concise summary of the physics governing electrospraying [25]. Bulk forces that are important to electrospraying include electrodynamic forces (proportional to the electric fields induced by the charged nozzle and emitted droplets), gravity, inertia, and drag force (proportional to jet velocity and the viscosity of the gas surrounding the jet). Surface stresses deforming the jet and acting against surface tension include electrodynamic stress (proportional to the charge density on the surface of the jet, and on the local electric field), pressure differential across the jet-air interface, and stresses due to liquid dynamic viscosity and inertia. For droplets emitted from a Taylor cone-jet, the following scaling relation has been developed:

$$d=\alpha\frac{Q^{aQ}\varepsilon_0^{a\varepsilon}\rho_l^{a\rho}}{\sigma_l^{a\sigma}\gamma_l^{a\gamma}},$$

d: droplet diameter, Q: volume flow rate, ε_0: permittivity of free space, ρ_l: liquid density, σ_l: liquid surface tension, γ_1: liquid bulk conductivity, and α: a coefficient depending on liquid permittivity. The remaining coefficients vary with different studies [25]:

Authors	aQ	aε	aρ	aσ	aγ
Fernandez de la Mora and Loscertales [26]	$\frac{1}{3}$	$\frac{1}{3}$	0	0	$\frac{1}{3}$
Gañan-Calvo [27] and Gañan-Calvo *et al.* [28]	$\frac{1}{2}$	$\frac{1}{6}$	$\frac{1}{6}$	$\frac{1}{6}$	$\frac{1}{6}$
Hartman *et al.* [29]	$\frac{1}{2}$	$\frac{1}{6}$	$\frac{1}{6}$	$\frac{1}{6}$	$\frac{1}{6}$

This relationship has been experimentally verified for both monoaxial [30] and coaxial electrospraying. One notable exception is the coaxial electrospraying of a charged ethylene glycol shell and an uncharged oil core, where a linear dependence of particle diameter on flow rate is observed [31]. This is an interesting result in that its deviation from the given power law

suggests that selective charging of one of the coaxial solutions can provide another level of control to achieve desired particle sizes.

The creation of fibers by electrospinning occurs in a process similar to electrospraying [32]. Electrostatic repulsion at the surface of a drop of liquid exiting a small capillary opposes surface tension to deform the drop into a Taylor cone. If a large voltage is applied to the nozzle, a jet escapes and travels toward a grounded collector. Steady-state equations describing the jet diameter, velocity, surface charge density, current, and electric field have been developed [33]. These equations reveal that the jet diameter is strongly dependent on the surface charge density and the local electric field. As charge quickly migrates to the jet surface upon exiting the nozzle both of these quantities reach their maximum value, leading to rapid thinning of the jet. Beyond this rapidly thinning region, a scaling relation has been developed to describe the decreasing diameter of the jet [32]:

$$d=\left(\frac{Q^3\rho}{2\pi^2 E_\infty I}\right)^{\frac{1}{4}} z^{-\frac{1}{4}},$$

d: jet diameter, Q: flow rate, ρ: fluid density, E_∞: applied field strength, and z: axial coordinate. Low flow rates, low fluid viscosities, and high applied field strengths are therefore expected to produce the smallest fiber diameters. He and Liu present a succinct discussion of other analytical methods used to model electrospinning [34].

There is a range of nozzle voltages and flow rates where electrospinning/electrospraying is stable. High fluid viscosity and density (inertia) slow the development of instabilities [32]. The most important instabilities in electrospinning are the whipping (for an excellent video refer to [35]) and axisymmetric Rayleigh (droplet formation) modes [36]. Perturbative stability analysis performed on the thin jet predicts that the whipping mode dominates for large surface charge and jet diameters [36]. Selection of spinning parameters favorable for the whipping instability is preferred for generation of contiguous fibers. Good fiber contiguity is particularly important in coaxial electrospinning of core-shell fibers for controlled drug release.

3. Fabrication technique/controlled release of drugs

3.1 Electrospinning

The techniques involved in electrospinning/electrospraying have been discussed in detail by excellent review articles [32,37–39]. For the sake of brevity we will be discussing co-axial electrospinning while drawing parallel with traditional mono-axial electrospinning wherever needed. The emergence of co-axial electrospinning has allowed the development of many new designs of functional nano-technological materials. Co-axial electrospinning is a simple and rapid technique to produce micro/nanotubes [40,41], drug- or protein-embedded nanofibers [42–44] and hybrid core-shell nanofibrous materials [45–50]. Figure 1 displays various scanning electron microscopy (SEM) images of the different morphologies of core-shell electrospun fibers. Figure 1a and b demonstrate the presence of core-shell feature in paclitaxel-loaded PLGA fibers designed to function as drug-eluting sutures. The electrospun fibers are capable of delivering paclitaxel over a period of 3 months but suffer from reduced mechanical properties [43,51,52]. Figure 1c–e illustrate the use of optical (c) and scanning electron microscopy (d–e) to visualize hollow core features of the microtubes produced from co-axial electrospinning using poly(caprolactone) as the shell and poly (ethylene oxide) as the core [40]. Dror *et al.* demonstrate control over the size distribution of the produced microtubes and transport of fluid inside the core of the fibers [40]. In our group, we have investigated the surface morphology and controlled release effect of added porogen (polyethylene glycol) in the shell of protein-loaded fibers. Figure 1f–h illustrate that fibers loaded with 0.07% wt./wt.

of PEG porogen (g) have an extensive amount of pore formation on day 30 compared to fibers without any porogen (f). Increasing the amount of porogen (7% wt./wt.) accelerates the degradation rate of the core-shell fibers (h).

The greatest advantage of co-axial electrospinning is its versatility in the type (hydrophobic or hydrophilic) and size (ranging from 100 nm to 300 μm) of fibers it can produce. Monoaxial electrospun fibers have been reported to be able to incorporate and release antibiotics, drugs and proteins in a sustained manner [53–58]. However, the distribution and release of drugs from the fibers are poorly controlled. Moreover, growth factors and cytokines embedded in polymer matrixes also suffer from significant decrease in bioactivity [58,59]. As delivery system for tissue engineering, co-axial electrospun fibers offer better drug stability, more complete drug encapsulation, and tighter control of release kinetics as compared to monoaxial fibers. Co-axial electrospinning circumvents technical limitations of monoaxial electrospinning by its core-shell design, allowing cytokines and growth factors to be dissolved in aqueous solution for encapsulation. Encapsulated lysozyme and platelet derived growth factor-bb released from core shell nanofibers have maintained high bioactivity over a period of 1 month [44,60]. The core-shell design also allows better control over the release kinetics of the drug of interest due to an increased number of variable parameters. Changes in the shell and core material properties via variation in molecular weight, polymer type and addition of porogen can fine-tune the release profile [44,61]. The following sections introduce the methods and parameters involved in co-axial electrospinning, as well as describe how varying production parameters can affect the controlled release of drugs.

The concepts of mono/co-axial electrospinning and electrospraying are similar, regardless of variations in experimental setup. As illustrated in Figure 2a, a polymer solution is dispensed through a needle using a syringe pump. Usually a high voltage DC supply is connected to the needle to provide a charging potential. When the electrostatic force induced by the charge potential overcomes the surface tension of the polymer solution, the droplet deforms into a Taylor cone [62, 63]. From the tip of the cone the polymer solution accelerates towards the nearest ground in the form of a jet. During the flight polymer solution is subject to shear and bending instabilities while the polymer solvent evaporates. The evaporation of solvents during flight, along with polymer concentration and molecular weight are the main factors controlling the size and shape of the product. In co-axial electrospinning (Figure 2b), two needles of different gauge size are arranged co-axially to dispense two different solutions concurrently. Depending on the solvents used, the two solutions can either mix or phase-separate at the needle. Similar to mono-axial electrospinning, electrostatic force induced by the high charging potential shears the core-shell droplet into polymeric co-axial fibers. Figure 3a illustrates the development of a Taylor cone with core-shell morphology and a gelled interface between the two solutions during electrospinning [40]. The following sections discuss various co-axial electrospinning parameters that can influence the formation of core-shell fibers and govern the kinetics of drug delivery.

3.1.1 Electrospinning parameters

3.1.1.1 Setups: A common co-axial electrospinning setup entails the use of a custom-designed spinneret to house the co-axial needles [64–67]. Shell and core solutions are connected to the spinneret with tubing and can be driven by separate syringe pumps [41,64,68] or pressurized gas [60,66]. The spinneret systems used in most works are set up to electrospin vertically with the spinning wheel at a fixed distance below the needle to collect the electrospun fibers. We have used a different setup which involves the assembly of a syringe inside another syringe setup (Figure 2b). The setup allows the dispension of shell/core solutions to be separately controlled by syringe pumps. The purpose of this design is to minimize loss of solution in the dead space of the connecting tubings and spinnerets, thereby allowing the encapsulation of

small fluid volumes (50 – 100 μL). Furthermore, we have opted to arrange the set up to electrospin horizontally rather than vertically to eliminate the possibility of the spinning wheel collecting imperfect products from the nozzle.

3.1.1.2 Polymer types, molecular weight and concentration: Polymer type, molecular weight, and concentration are three crucial factors that determine the feasibility of electrospinning. The types of polymer amenable to electrospinning can be classified by their hydrophilicity. Hydrophilic polymers (e.g. polysaccharides) or extracellular-matrix proteins (e.g. collagen and hyaluronic acid) have been processed into electrospun fibers by dissolving the polymers in water, strong acids or a mixture of water and polar organic solvents [69–75]. Electrospinning of collagen and polysaccharide polymers are covered in detail in this issue by Dr. Bowlin and Dr. Park, respectively. Hydrophobic polymers such as poly(caprolactone) or poly(lactic-co-glycolic acid) are dissolved in organic solvents [42,44]. The use of different solvents and their effects on co-axial electrospinning is covered below in Section 3.

Changes in polymer concentration and molecular weight affect the viscosity and surface tension of the solution, and therefore greatly influence the electrospun product. Doshi *et al.* establish that the ideal viscosity for an electrospinning solution ranges from 800 to 4000 centipoises [38,63].This viscosity range is ideal for supporting initial jet stabilization and subsequent jet thinning. Solutions below 800 centipoises are too dilute to undergo chain entanglement and prone to breakup into droplets [63]. On the other end of the spectrum, it is difficult for the applied charged potential to overcome the surface tension of viscous solutions above 4000 centipoises. Operating within the acceptable range of viscosity, it is typical to collect electrospun fibers ranging from 100 nm to 300 μm in diameter. The diameter of the electrospun fibers correlates directly with both polymer concentration and molecular weight. Near the lower viscosity limit, the electrospun fibers are more prone to forming micron-sized beads on the fibers [56]. The upper and lower limits for polymer molecular weight vary greatly, and depend on the polymer type and entanglement behavior.

3.1.1.3 Solvent properties: While the type of polymer determines the type of solvent used in the electrospinning process, different solvent properties play a crucial role in fiber formation. Three important characteristics of solvents to consider in the co-axial electrospinning process are surface energy, volatility, and miscibility. The surface energy of the solvent influences the ability of the applied electrical potential to shear the polymer solution into electrospun fibers. For example, chloroform (a common solvent for hydrophobic polymers) has a surface tension of 26 mN/m, while water (used for hydrophilic polymers) has a value of 72 mN/m. This solvents' surface tension disparity explains why poly(caprolactone) (PCL) dissolved in chloroform can be electrospun more readily as compared to chitosan dissolved in water. The high surface tension also causes more instability and resulted in a broad range of chitosan fiber diameters [38].

Solvent volatility is critical in determining whether sufficient solvent evaporation can occur in the flight of the fiber between the needle and its designated ground. The high boiling point of water (100°C) compared to chloroform (61°C) or dichloromethane (40°C) necessitates additional drying for electrospinning of hydrophilic polymers. Insufficient solvent evaporation will lead to formation of ribbon-like fibers or fiber fusion [38]. On the other hand, if solvent volatility is too high then it may lead to the drying of the jet even before jet whipping can thin the fiber. This in turn leads to the formation of large diameter fibers. Within optimum range of solvent volatility, fiber diameter has an inverse relationship with it. Drastic difference in solvent volatility introduces an extra level of difficulty for co-axial electrospinning. We observed this phenomenon in comparing the electrospun product of PCL dissolved in either chloroform or dichloromethane as the shell solution and deionized water as the core solution. The greater solvent volatility disparity between dichloromethane and water resulted in

increased solvent separation and separation of shell/core solution as compared to co-axial electrospinning with chloroform and water.

Solvent miscibility is another parameter to consider in order to ensure consistent core-shell electrospun fiber products. In our study of electrospinning with chloroform and water, the poor solubility of chloroform in water (0.815%) leads to uneven distribution of water inside the fiber and increases the probability of fiber defects (pendant droplets of a mixture of core-shell solution). However, when a secondary solvent such as ethanol is added in chloroform, the occurrence of electrospinning defects is much reduced and resulted in an even distribution of water inside the fiber. Ethanol (or methanol) is an excellent intermediate solvent because of its good miscibility in chloroform and water, as well as its low surface energy (22 mN/m) and boiling point (78°C). Confocal images presented in Figure 4 offer a comparison between fluorescein isothiocyanate-bovine serum albumin (FITC-BSA) mixed into the polymer solvent vs. FITC-BSA encapsulated via co-axial electrospinning. FITC-BSA mixed with poly-caprolactone (PCL) and poly(ethyl ethylene phosphate) (PCLEEP) copolymer solution in dichloromethane and electrospun shows uneven distribution of FITC-BSA throughout the fiber and decrease in fluorescent intensity (Figure 4a) [58]. On the other hand, FITC-BSA distribution within co-axially electrospun fibers is uniform (Figure 4b), which would lead to more controllable release kinetics.

3.1.1.4 Voltage: Electrical gradient is the driving force of the electrospinning process. An insufficient electrical charge potential cannot overcome the surface tension of the polymer drop to form electrospun fibers. Electrospinning of monoaxial fibers begins to proceed at an electrical field above 0.3 kV/cm, and an increasing field strength will significantly reduce the fiber size [56]. Above 1.2 kV/cm, the increasing field strength ceases to have a size-reducing effect and instead introduces more fiber size variability due to increasing jet instability [56]. Electrospun fibers of polyethylene oxide (PEO) show an increase in the extent of beaded-fiber defect when electrospinning is conducted outside the range of optimal field strength (between 0.5 to 1 kV/cm) [77]. Co-axial electrospinning typically can be achieved at similar field strength as monoaxial electrospinning, depending on the solvent miscibility and surface tension of the core/shell solutions. Poor miscibility between core/shell solutions (e.g. water and chloroform) requires higher field strengths to overcome the solution surface tension; improving the solution miscibility (by adding secondary solvent to the shell solution) not only reduces the necessary applied voltage but also improves the fiber size uniformity.

3.1.1.5 Flow rate ratio: The ratio of flow rates between the core and shell solutions profoundly affects the quality of the product of co-axial electrospinning. Figure 3b is a representative illustration of the effect of variation in flow rate ratio during co-axial electrospinning using poly(caprolactone) in the shell (75/25 volume ratio of chloroform/ethanol) and 4% wt/wt FITC-BSA in the core (dissolved in water). At flow rate ratios less than 1:2 (core:shell), there is insufficient shell solution to encapsulate the core solution. The resulting core/shell solutions form pendant drops at the needle, projecting only droplets under electrical gradient. For increased shell flow rate (flow rate ratios between 1:2 and 1:3), there is occasional encapsulation of the core solution into core/shell electrospun fibers although most of the product formed in this condition remains as solution-mixture droplets. Flow rate ratios between 1:3 and 1:6 allow the formation of stable core/shell Taylor cones and yield consistent electrospun core-shell fibers. Further increasing the shell flow rate (ratio from 1:7 to 1:10) does not change the ability of the core/shell solutions to be electrospun, but reduces the encapsulation efficiency of the core solution. Li *et al.* study the electrospinning of a poly(vinyl pyrrolidone) (shell) and tetraethyl orthosilicate (core) to efficiently produce polymer nanotubes [78]. Fixing the outside flow rate, they report that increasing core flow rate not only increases both the core and overall fiber size but also reduces the fiber wall thickness. Interestingly, Dror *et al.* keep

the same flow rate ratio but find that the core size increases with the electrical conductivity of the core solution [40].

3.1.1.6 Other parameters: Electrospinning distance, temperature and humidity are additional parameters that affect the size and morphology of the electrospun product. Electrospinning distance can influence fiber size and determine the final product morphology. Increasing electrospinning distance yields fibers of smaller size. However, a capillary-to-collector distance greater than 20 cm will lead to significant fiber loss to the surroundings as the electrospinning jet seeks the nearest ground on which to deposit [63]. Conversely, when there is inadequate electrospinning distance the electrospun fibers are more prone to fusion, as there can be residual organic solvent present during fiber deposition [79]. Temperature and humidity also affect the electrospun product morphology. Temperature elevation increases molecular mobility which in turn increases the solution conductivity while decreasing solution viscosity and surface tension. These conditions are favorable for decreasing the diameter of the electrospun fibers [80,81]. Furthermore, this tend to decrease the crystallinity and increase the surface roughness of the electrospun product [80,81]. Increase in relative humidity in the electrospinning chamber decreases the evaporation rate of polymer solvents and results in larger electrospun fiber diameters [76]. Kim *et al.* also report significant pore formation on the electrospun polystyrene fibers at a relative humidity of 30% [76]. Due to the multitude of modifiable parameters in the electrospinning process, distance, temperature, and humidity are typically kept constant to enhance the reproducibility of the electrospun product. Important parameters known to influence the electrospining/spraying process are summarized in Figure 5. It is important to stress that these parameters are not mutually exclusive. Even their relationship with fiber diameter holds true only within an optimum range, often dictated by practical considerations. To support the above contentions it can be cited that applied voltage is related to the electrospinning/spraying distance through the parameter of electric field strength. Fiber diameter has an inverse relation with electric field strength. However, very high voltages cannot be pursued because of the onset of undesirable jet instability and also concerns for safety and potential damage to the drug. Therefore, in realistic terms these parameters can be varied only within some finite range to obtain fibers/particles of desirable diameter, shape and texture.

3.1.2 Controlled release through core-shell electrospun fibers—Core-shell electrospun fibers are generally designed to concentrate the drug in the core of the fibers as opposed to randomly distributing the drug throughout the fiber matrix. A simplified summary of the various parameters and their effects on drug release can be found in Table 1.

Using poly(caprolactone) and poly(methylmethacrylate) (PMMA) as carriers and rhodamine 610 dye as a model drug, Srikar *et al.* investigate the effect of varying polymer type (PCL vs. PMMA), polymer concentration (11, 13 and 15%) and molecular weight (120, 350 and 996 kDa) [61]. As expected, increase in polymer concentration and molecular weight both reduces the rate at which the rhodamine dye is released from the fiber. Srikar *et al.* suggest that both increase in concentration and molecular weight increase the fiber shell density, thus resulting in a higher controlled release barrier [61]. Other groups have also reported that the increase in polymer concentration can delay the release of drugs such as paclitaxel and tetracycline hydrochloride [42,64]. However, another factor to consider is the possible changes in the fiber diameter as a result of alterations in concentration and molecular weight, which can be a confounding factor affecting the drug release kinetics.

The strength of the polymer-drug interaction is another variable that greatly influences the extent of drug release. Hydrophilicity, charge density, and degradability are characteristics of a polymer carrier that can play roles in its interaction with the drug of interest. Srikar *et al.* report that PMMA has greater affinity to rhodamine dye than PCL, leading to a much slower

release rate from PMMA than from PCL nanofibers [61]. A notable variable introduced in their work involves forming PCL (shell)/PMMA (core) fibers, and modulating the concentration of PMMA to significantly influence the rate of rhodamine being released [61]. Kraitzer *et al.* correlate the degradability of different blends of poly(lactic-glycolic acid) (75/25 vs. 50/50 PLGA) and the resulting influence on the release kinetics of paclitaxel [51,52]. Increasing the degradation rate by increasing the ratio of fast-degrading PGA resulted in a faster release of paclitaxel (80% in 40 weeks vs. 30% with 75/25 PLGA). In addition, as with all other reservoir-type systems, increase in encapsulated drug concentration leads to a higher diffusive driving force for drug release [43]. Control of drug release by varying polymer-drug interactions can be an empirical process, as the degree of interaction varies greatly depending on the types of polymers and drugs being used.

The use of a porogen in the shell phase of core-shell electrospun fibers as a way to modulate drug release kinetics have been investigated by several groups [44,60,67]. Polyethylene glycols are interesting for their low cytotoxicity, high water solubility and fast *in vivo* clearance through the kidney. Increase in the amount of incorporated porogen leads to significant fiber swelling and pore formation [44,82].

Flow rate ratio and scaffold porosity are other parameters that can be changed to fine-tune drug release kinetics. In varying the flow rate ratio of PCL (shell) and BSA (core) solutions, Jiang *et al.* report poor encapsulation with flow rate ratio near 1:1 and decreased release rate of BSA with reduced core flow rate [60]. It can be speculated that increasing the flow rate ratio (shell:core) would lead to a reduction of drug concentration in the core, thus leading to a slower release kinetics. Lastly, Zilberman *et al.* use freeze drying or an inverted emulsion technique to increase the shell polymer porosity to facilitate drug release [42].

3.2 Electrospraying

Unlike electrospinning, electrospraying results from the interaction of bulk and surface electrohydrodynamic forces breaking the jet into droplets. Due to surface tension the jet fragments subsequently acquire a spherical shape before being deposited on a grounded substrate. Like electrospinning this process is also affected by a multitude of parameters. An increase in the magnitude of electrospraying parameters like voltage [83], conductivity [84] and surface tension [29,85] of sprayed solution is associated with a decrease in particle diameter. Whereas an increase in the magnitude of electrospraying parameters like flow rate [30], density [29,85] and viscosity [86] of sprayed solution is associated with an increase in particle diameter. Although variation of nozzle size has generally been found to have a direct relation with particle diameter, this opinion is not universally shared [87]. Furthermore, decreasing the flow rate [30] and solvent evaporation rate [30] can lead to the fabrication of particles with spherical morphology and smooth texture.

A large portion of current literature in electrospraying deals with applications such as microelectronics, sensing and chemical analysis. It is only recently that researchers apply this technique to drug delivery. The following techniques have either been applied or can be potentially applied for loading drug into the sprayed vehicle.

Adsorption—In the adsorptive technique, drug is adsorbed onto the sprayed carrier by exposing the carrier to a drug solution. A major drawback is that most of the drug is often loosely attached and consequently there is a prominent burst release. The period of sustained release also tends to be short for such DDS.

Encapsulation—Encapsulation can be achieved by several methods.

a. Collision of droplets of opposite polarity: In this process two polymeric jets and the droplets emanating from them bear opposite charges. As droplets are emitted from two adjacent capillaries connected to opposite charges they attract one another due to columbic forces and subsequently fuse (Fig.6a). Therefore, drug encapsulation is possible if one charged species is polymer and the oppositely charged species is the drug [88].

b. Electrospraying of a drug dissolved/suspended in polymer solution with solidification by evaporation: The drug-polymer solution is sprayed and the solvent is evaporated as the jet travels towards the collecting plate. Thus, the drug gets encapsulated in the dried polymer (Fig.6b) [89].

c. Electrospraying of a drug dissolved/suspended in polymer with solidification by a chemical or ionic crosslinker: The drug-polymer solution is sprayed into a bath containing a crosslinker which binds the polymer in the droplet. This leads to the drug becoming entrapped in the particulate polymeric network (Fig.6c) [90].

d. Coaxial Electrospraying: This process is similar to coaxial electrospinning described in detail in the preceding section. This process holds immense potential as the core-shell structure will reduce any burst release and may achieve a near zero order release kinetics. Moreover it consumes less time to fabricate and has high encapsulation efficiency and loading capacity (Fig.6d) [91].

4. Applications

Discussing the entire gamut of drug delivery applications of these vehicles is beyond the scope of this review. Instead we will highlight a few potential applications reinforced with relevant examples from the literature. These delivery vehicles are in their early stages of development, therefore few *in vivo* experiments having been performed and the delivery efficiency of many of these devices has been demonstrated only by model drugs.

4.1 Tissue engineering

4.1.1 Electrospinning

4.1.1.1 Protein delivery: Chew *et al.* encapsulate human nerve growth factor (hNGF) along with BSA as a carrier protein into nanofibers composed of a copolymer of poly(ε-caprolactone (PCL) and poly(ethyl ethylene phosphate) (PCLEEP) [58]. The protein was uniformly dispersed in the polymer solution as aggregates. The induction of PC12 cells into the neuronal lineage by the released hNGF indicates a partial retention of the bioactivity of the growth factor in the electrospinning process. A sustained release of hNGF through three months is demonstrated, albeit of reduced bioactivity towards the end of release. The same group demonstrates the delivery of human glial cell-derived neurotrophic factor (GDNF) from a similar polymeric nanofibrous platform for peripheral nerve regeneration in a sciatic model in rats. The nanofibers are aligned in the lumen of the nerve conduit to purportedly provide topographical guidance to the regenerating neurons. Highest functional and morphological recovery is observed in the group treated with longitudinally aligned fibers eluting GDNF, sustained over a period of 2 months [59]. Casper *et al.* incorporate low molecular weight heparin (LMWH) or its conjugated form with PEG in fibers spun from 10 wt % poly(ethylene oxide) (PEO) or 45 wt % poly(lactide-*co*-glycolide) (PLGA) [92]. Heparin is included to take advantage of its high affinity with a host of growth factors such as fibroblast growth factor (FGF), vascular endothelial growth factor (VEGF), heparin-binding epidermal growth factor (HBEGF), and transforming growth factor-β (TGF-β). PEG improves the retention of heparin within the fibers to achieve a sustained release over 14 days. Li and coworkers fabricate nanofibers from an aqueous solution of silk protein, BMP-2 and nanoparticles of hydroxyapatite. They observe a pro-osteogenic effect on hMSCs seeded onto the fibrous

scaffold. The combined presence of BMP-2 and hydroxyapatite lead to maximum *in vitro* bone formation as confirmed by enhanced mineralization and BMP-2 transcript expression [93].

Liao *et al.* demonstrate the incorporation of PEG into the shell of PCL nanofibers to regulate the release of the encapsulated proteins in the core [44]. A near zero-order release of platelet derived growth factor-bb (PDGF-bb) can be produced with no associated burst release. In addition, aligned PDGF-bb loaded nanofibers are fabricated. These aligned drug-loaded fibers may simultaneously provide biochemical and topographical cues to the seeded cells, provisions that should prove beneficial for many tissue engineering applications. The released PDGF-bb maintained its bioactivity throughout the release period, at least partially, as demonstrated by a proliferation assay on NIH 3T3 cells.

4.1.1.2 Nucleic acid: Luu *et al.* describe the encapsulation of plasmid DNA in a PLA–PEG block copolymer nanofibrous matrix for tissue engineering purposes [94]. Approximately 80% of the β-galactosidase reporter gene is released in 20 days. Transfection experiments performed on the osteoblastic cell line MC3T3-E1 demonstrate increased transfection efficiency of the fiber-encapsulated DNA over naked plasmid added to the medium, but lower than that with a commercial transfecting reagent. For improving stability of DNA during the electrospinning process Liang *et al.* have incorporated solvent-induced compacted DNA in PLA-PEG-PLA triblock copolymer [95]. The non-woven nanofiber mats produce a significant improvement on transfection efficiency when the cells are directly seeded onto the scaffold. In a similar effort, Nie *et al.* design a composite nanofibrous scaffold with DNA (BMP-2 plasmid DNA)/ chitosan nanoparticles dispersed in PLGA/hydroxylapatite (HAp) matrix for bone tissue engineering.

4.1.2 Electrospraying

4.1.2.1 Protein: Xu and his colleagues have studied the encapsulation of BSA in electrosprayed particles generated from chitosan [90] and poly(lactide) (PLA) [96]. In one study, the chitosan in sprayed particles is cross-linked by tripolyphosphate. In the other study, BSA is loaded into particles by electrospraying an emulsion of BSA in a PLA solution. The release rate of BSA from chitosan particles reaches a steady state within 24 hours, whereas the release of BSA from the PLA particles never reaches steady state within the time of observation. The authors speculate that this is due to the erosion of PLA. It appears that the chitosan system is more advantageous because of the milder processing conditions, lack of organic solvent, and absence of emulsifier.

4.2 Delivery of chemotherapeutic agents

4.2.1 Electrospinning—Nanofibers have been used sparingly as an anti-neoplastic drug delivery device. This has to do with the nature of fibrous scaffolds, which permit delivery only after tumor resection and surgical implantation of the device. The majority of nanofiber antineoplastic agent delivery systems have been envisioned for the treatment of malignant gliomas (a type of brain tumor). The current DDS of choice is post tumor-resection implantation of a drug-eluting wafer. Thus, all these studies have tried to elucidate the benefits of implanting a nanofiber delivery system over a wafer-based system. In one study 1,3-bis(2-chloroethyl)-1-nitrosourea (BCNU, an anti-neoplastic agent extensively used to treat malignant glioma) is encapsulated by Xu *et al.* in PEG–PLLA diblock copolymer fibers [97]. The BCNU released from the fibers retains its efficacy for prolonged periods as compared with pristine BCNU. This is reflected in the decreasing viability of rat glioma C6 cells over prolonged periods in an *in vitro* viability assay. Proposing an alternative drug delivery device for post-surgery glioma management, Xie *et al.* have also used the platform of PLGA nanofibers to deliver paclitaxel, an antineoplastic drug [54]. A sustained release of paclitaxel over 2 months is demonstrated. This represents a distinct advantage when compared to the release of BCNU from wafers which

lasts only a period of days. In another strategy, doxorubicin hydrochloride (Dox), a hydrophilic anti-neoplastic agent is electrospun as an aqueous emulsion in a solution of PEG-PLLA copolymer [98]. This method affords uniform distribution of the drug within the fiber and a diminished burst release.

4.2.2 Electrospraying—Wu and coworkers successfully encapsulate doxorubicin inside electrosprayed particles of temperature-responsive, genetically engineered elastin-like polypeptides (ELP) [89]. A high 20 w/w % loading of doxorubicin does not appreciably alter the particle dimension and shape. The pH-regulated tuning of ELP solubility could lead to a controlled release of the drug over desired periods.

4.3 Wound management devices

4.3.1 Electrospinning—Nano-fibers are good candidates for wound dressing due to their high porosity, which allows exchange of gases, moisturization of the wound, and drainage of exudates from the wound site. The large surface area of nanofibers can lead to high absorption of exudates. Sub-micron inter-fiber porosity on the other hand can block entry of bacteria into the wound site. Thus, nanofibrous dressings can substantially decrease the risk of wound infection. Good flexibility of the dressing and high mechanical strength is also ideal for meeting protective requirements. In addition, the fibers can control the release of various wound-healing drugs, proteins and antibiotics [99]. In a study by Choi *et al.* recombinant human epidermal growth factor (EGF) is chemically conjugated to the electrospun nanofiber surface via amine-terminated PEG linker [100]. The nanofibers were spun out of poly(e-caprolactone) (PCL) and PCL–PEG block copolymers. Culture of keratinocytes on this nanofiber surface demonstrates an enhanced expression of keratinocyte-specific genes. This system affords better wound healing for the initial 7 days as compared to the controls in a dorsal wound-healing model of diabetic mice. Immunohistochemical staining at 14 days demonstrates an increased expression of EGF-receptor (EGFR) in re-epithelized tissue lining the wound site.

Intra-abdominal injury is often associated with fibrin exudation, infection, and inflammation which ultimately leads to varying levels of peritoneal adhesion formation. These adhesions are undesirable as they render the intra-abdominal organs inaccessible in case of future surgery and are notorious as a source of intestinal strictures and consequent obstruction. Bolgen *et al.* have performed *in vivo* studies to elaborate the effect of ornidazole-releasing nanofibrous DDS on intra-abdominal healing. Ornidazole, an antibiotic with activity against intestinal anaerobic bacteria is adsorbed onto PCL nanofibrous membranes [101]. In a rat model of intra-abdominal injury, gross anatomical and microscopic studies suggest that adhesion formation is reduced considerably in the treatment group. Even when adhesions were formed they are loose and easy to remove. Maximum benefit in terms of the rate and quality of healing is obtained when antibiotic release is combined with the nanofibrous barrier. In other notable studies in the field of burn/wound dressing, Katti and his colleagues have demonstrated the ability to electrospin cefazolin dissolved in a solution of PLGA in THF + DMF [56]. Kim *et al.* have probed the controlled release of a hydrophilic antibiotic Mefoxin® (cefoxitin sodium) from electrospun nanofibers composed of PLGA and PEG-b-PLA [102]

Huang and coworkers have encapsulated resveratrol and gentamycin sulfate in the core of PCL core-shell nanofibers [103]. Release of drugs from the core is mediated through the biodegradation of PCL by *Pseudomonas* lipase. Sustained release is observed for 7 days with no initial burst release.

4.3.2 Electrospraying—Ampicillin, an antibiotic which has a broad-spectrum activity against Gram-positive and some Gram-negative bacteria has been encapsulated by Arya *et al.* in chitosan nanospheres generated through electrospraying [104]. They optimize several

electrospraying parameters to obtain particles with a narrow particle size distribution and a high encapsulation efficiency of 80.4%. Efficacy of the released ampicillin is confirmed by a zone of inhibition in ampicillin-sensitive E. coli colonies grown on agar.

5. Conclusion

Electrohydrodynamic techniques are promising tools for fabricating DDS. Incorporation of drug into the delivery vehicle is usually a one-step process. High loading capacity, high encapsulation efficiency, simultaneous delivery of topographical and biochemical cues, ease of operation, and cost-effectiveness comprise other appealing features. As therapeutics like siRNA, aptamer, antigen molecules gain increasing prominence in the near future, opportunities for electrohydrodynamics-generated DDS will continue to flourish. To make this tool more effective, a better understanding of the underlying physics will improve the control of the electrospun and electrosprayed products. Sometimes it is difficult to reproduce results reported in the literature; part of the problem lies with a plethora of setup conditions. A clearer reporting of the experimental conditions and better awareness of the important determinants will have a positive impact in overcoming this impediment. Novel designs to produce a co-electrospinning apparatus which is efficient, easy to handle, and at the same time reduces the dead space through which the polymer and the drug has to travel before entering into the coaxial mode would be valuable. Methodologies to increase the jet stability also warrant further development. Successful generation of stable and uniform jets will lead to near mono-dispersed fibers or particles and better repeatability and reproducibility. Concerns still linger about the extent to which protein or DNA can maintain their structure under the influence of high voltage. However, recent evidence demonstrates that cells which are electrosprayed retain their viability, suggesting that the effects of high voltage on protein/DNA structure and function may be temporary [105]. This may also be ameliorated by an approach of using AC voltage to carry out the electrospinning/spraying, which requires a relatively low voltage and eliminates residual charge on the resultant particles and fibers [106]. To solidify the evidences for efficacy of these electrohydrodynamic methods and the resultant DDS, more *in vivo* animal studies need to be carried out. If implemented, the above measures will surely go a long way to establish electrospraying and electrospinning as methods par excellence in the field of DDS fabrication.

Acknowledgements

Support to this work by NIH (EB003447) is acknowledged.

References

1. Moghimi SM, Hunter AC, Murray JC. Nanomedicine: current status and future prospects. The FASEB journal 2005;19:311–330. [PubMed: 15746175]
2. Goldberg M, Langer R, Jia X. Nanostructured materials for applications in drug delivery and tissue engineering. J Biomater Sci Polym Ed 2007;18:241–268. [PubMed: 17471764]
3. Sokolsky-Papkov M, Agashi K, Olaye A, Shakesheff K, Domb AJ. Polymer carriers for drug delivery in tissue engineering. Adv Drug Deliv Rev 2007;59:187–206. [PubMed: 17540473]
4. Murugan R, Ramakrishna S. Design strategies of tissue engineering scaffolds with controlled fiber orientation. Tissue Eng 2007;13:1845–1866. [PubMed: 17518727]
5. Quaglia F. Bioinspired tissue engineering: The great promise of protein delivery technologies. Int. J. Pharm 2008;364:281–297. [PubMed: 18538517]
6. Saltzman WM, Olbricht WL. Building drug delivery into tissue engineering. Nat.Rev. Drug. Discov 2002;1:177–186. [PubMed: 12120502]
7. Greiner A, Wendorff JH, Yarin AL, Zussman E. Biohybrid nanosystems with polymer nanofibers and nanotubes. Appl. Microbiol. Biotechnol 2006;71:387–393. [PubMed: 16767464]

8. Vasita R, Katti DS. Nanofibers and their applications in tissue engineering. Int. J. Nanomedicine 2006;1:15–30. [PubMed: 17722259]
9. Kimizuka N. Self-Assembly of Supramolecular Nanofibers. Adv. Polymer Sci 2008;219:1–26.
10. Ma PX, Zhang R. Synthetic nano-scale fibrous extracellular matrix. J. Biomed. Mater. Res 1999;46:60–72. [PubMed: 10357136]
11. De Jong WH, Borm PJ. Drug delivery and nanoparticles: Applications and hazards. Int. J. Nanomedicine 2008;3:133–149. [PubMed: 18686775]
12. Kingsley JD, Dou H, Morehead J, Rabinow B, Gendelman HE, Destache CJ. Nanotechnology: a focus on nanoparticles as a drug delivery system. J. Neuroimmune. Pharmacol 2006;1:340–350. [PubMed: 18040810]
13. Zambaux MF, Bonneaux F, Gref R, Maincent P, Dellacherie E E, Alonso MJ, Labrude P, Vigneron C. Influence of experimental parameters on the characteristics of poly(lactic acid) nanoparticles prepared by a double emulsion method. J. Control. Release 1998;50:31–40. [PubMed: 9685870]
14. Jain R. The manufacturing techniques of various drug loaded biodegradable poly(lactide-co-glycolide) (PLGA) devices. Biomaterials 2000;21:2475–2490. [PubMed: 11055295]
15. Allemann E, Gurny R, Doelker E. Preparation of aqueous polymeric nanodispersions by a reversible salting-out process: influence of process parameters on particle size. Int. J. Pharm 1992;87:247–253.
16. McCarron PA, Donnelly RF, Marouf W. Celecoxib-loaded poly(D,L-lactide-co-glycolide) nanoparticles prepared using a novel and controllable combination of diffusion and emulsification steps as part of the salting-out procedure. J. Microencapsul 2006;23:480–498. [PubMed: 16980271]
17. Bilati U, Allémann E, Doelker E. Nanoprecipitation versus emulsion-based techniques for the encapsulation of proteins into biodegradable nanoparticles and process-related stability issues. AAPS PharmSciTech 2005;6:E594–E604. [PubMed: 16408861]
18. Bodmeier R, Wang J. Microencapsulation of drugs with aqueous colloidal polymer dispersions. J. Pharmaceut. Sci 1993;82:191–194.
19. Katas H, Alpar HO. Development and characterisation of chitosan nanoparticles for siRNA delivery. J. Contr. Release 2006;115:216–225.
20. Mao HQ, Roy K, Troung-Le VL, Janes KA, Lin KY, Wang Y, August JT, Leong KW. Chitosan-DNA nanoparticles as gene carriers: synthesis, characterization and transfection efficiency. J. Contr. Release 2001;70:399–421.
21. Vehring R. Pharmaceutical particle engineering via spray drying. Pharm. Res 2008;25:999–1022. [PubMed: 18040761]
22. Soppimath KS, Aminabhavi TM, Kulkarni AR, Rudzinski WE. Biodegradable polymeric nanoparticles as drug delivery device. J. Contr. Release 2001;70:1–20.
23. Scholes P, Coombes AGA, Illum L, Davis SS, Davies MC. The preparation of sub-200 nm poly (lactide-co-glycolide) microspheres for site-specific drug delivery. J. Contr. Release 1993;25:145–153.
24. Wu Y, Clark RL. Electrohydrodynamic atomization: a versatile process for preparing materials for biomedical applications. J. Biomater. Sci. Polymer. Ed 2008;19:573–601.
25. Jaworek A, Sobczyk AT. Electrospraying route to nanotechnology: An overview. Journal of Electrostatics 2008;66:197–219.
26. De la Mora JF, Loscartales IG. The current emitted by highly conducting Taylor cones. J. Fluid Mech 1994;260:155–184.
27. Gañan-Calvo AM. New microfluidic technologies to generate respirable aerosols for medical applications. J. Aerosol Sci 1999;30:541–542.
28. Gañan-Calvo AM, Davila J, Barrero A. Current and droplet size in the electrospraying of liquids: Scaling laws. J. Aerosol Sci 1997;28:249–275.
29. Hartman RPA, Brunner DJ, Camelot DMA, Marijnissen JCM, Scarlett B. Jet break-up in electrohydrodynamic atomization in the cone-jet mode. J. Aerosol Sci 2000;31:65–95.
30. Yao J, Lim LK, Xie JW, Hua JS, Wang CH. Characterization of electrospraying process for polymeric particle fabrication. J. Aerosol Sci 2008;39:987–1002.
31. Lopez-Herrera JM, Barrero A, Lopez A, Loscertales IG, Marquez M. Coaxial jets generated from electrified Taylor cones. Scaling laws. J. Aerosol Sci 2003;34:535–552.

32. Rutledge GC, Fridrikh SV. Formation of fibers by electrospinning. Adv. Drug.Deliv. Rev 2007;59:1384–1391. [PubMed: 17889398]
33. Feng JJ. The stretching of an electrified non-Newtonian jet: A model for electrospinning. Phys Fluid 2002;14:3912–3926.
34. He JH, Liu HM. Variational approach to nonlinear problems and a review on mathematical model of electrospinning. Nonlinear Analysis 2005;63:e919–e929.
35. Reneker DH, Yarin AL, Fong H, Koombhongse S. Bending instability of electrically charged liquid jets of polymer solutions in electrospinning. J. Appl. Phys 2000;87:4531–4547.
36. Shin YM, Hohman MM, Brenner MP, Rutledge GC. Electrospinning: A whipping fluid jet generates submicron polymer fibers. Appl. Phys. Lett 2001;78:1149–1151.
37. Moghe AK, Gupta BS. Co-axial electrospinning for nanofiber structures: Preparation and applications. Polymer Rev 2008;48:353–377.
38. Sill TJ, von Recum HA. Electro spinning: Applications in drug delivery and tissue engineering. Biomaterials 2008;29:1989–2006. [PubMed: 18281090]
39. Chew SY, Wen Y, Dzenis Y, Leong KW. The role of electrospinning in the emerging field of nanomedicine. Current Pharm. Design 2006;12:4751–4770.
40. Dror Y, Salalha W, Avrahami R, Zussman E, Yarin AL, Dersch R, Greiner A, Wendorff JH. One-step production of polymeric microtubes by co-electrospinning. Small 2007;3:1064–1073. [PubMed: 17315262]
41. Li S, Sun B, Li XR, Yuan XY. Characterization of electrospun core/shell poly(vinyl pyrrolidone)/poly(L-lactide-co-epsilon-caprolactone) fibrous membranes and their cytocompatibility in vitro. J. Biomater. Sci. Polymer. Ed 2008;9:245–258.
42. Zilberman M, Elsner JJ. Antibiotic-eluting medical devices for various applications. J. Contr. Release 2008;130:202–215.
43. Zilberman M, Kraitzer A. Paclitaxel-eluting composite fibers: Drug release and tensile mechanical properties. J. Biomed. Mater. Res 2008;84A:313–323.
44. Liao IC, Chew SY, Leong KW. Aligned core-shell nanofibers delivering bioactive proteins. Nanomedicine 2006;1:465–471. [PubMed: 17716148]
45. McCann JT, Li D, Xia YN. Electrospinning of nanofibers with core-sheath, hollow, or porous structures. J. Mater. Chem 2005;15:735–738.
46. McCann JT, Marquez M, Xia YN. Melt coaxial electrospinning: A versatile method for the encapsulation of solid materials and fabrication of phase change nanofibers. Nano Letters 2006;6:2868–2872. [PubMed: 17163721]
47. Dong H, Jones W. Preparation of submicron polypyrrole/poly(methyl methacrylate) coaxial fibers and conversion to polypyrrole tubes and carbon tubes. Langmuir 2006;26:11384–11387. [PubMed: 17154629]
48. Ma M, Krikorian V, Yu JH, Thomas EL, Rutledge GC. Electrospun polymer nanofibers with internal periodic structure obtained by microphase separation of cylindrically confined block copolymers. Nano Letters 2006;12:2969–2972. [PubMed: 17163741]
49. Jiang HL, Zhao PC, Zhu KJ. Fabrication and characterization of zein-based nanofibrous scaffolds by an electrospinning method. Macromolecular Bioscience 2007;7(4):517–525. [PubMed: 17429829]
50. Lagerwall JPF, McCann JT, Formo E, Scalia G, Xia Y. Coaxial electrospinning of microfibres with liquid crystal in the core. Chem. Comm 2008:5420–5422. [PubMed: 18985230]
51. Kraitzer A, Ofek L, Schreiber R, Zilberman M. Long-term in vitro study of paclitaxel-eluting bioresorbable core/shell fiber structure. J. Control. Release 2008;126:139–148. [PubMed: 18201789]
52. Kraitzer A, Zilberman M. Paclitaxel-loaded composite fibers: Microstructure and emulsion stability. J. Biomed. Mater. Res 2007;81A:427–436.
53. Buschle-Diller G, Cooper J, Xie ZW, Wu Y, Waldrup J, Ren XH. Release of antibiotics from electrospun bicomponent fibers. Cellulose 2007;14:553–562.
54. Xie JW, Wang CH. Electrospun micro- and nanofibers for sustained delivery of paclitaxel to treat C6 glioma in vitro. Pharm. Res 2006;23:817–1826.
55. Xie J, Tan RS, Wang CH. Biodegradable microparticles and fiber fabrics for sustained delivery of cisplatin to treat C6 glioma in invitro. J. Biomed. Mater. Res 2008;85A:897–908.

56. Katti DS, Robinson KW, Ko FK, Laurencin CT. Bioresorbable nanofiber-based systems for wound healing and drug delivery: Optimization of fabrication parameters. J.Biomed. Mater. Res. B. Appl. Biomater 2004;70B:286–296. [PubMed: 15264311]
57. Kumbar SG, Nair LS, Bhattacharyya S, Laurencin CT. Polymeric nanofibers as novel carriers for the delivery of therapeutic molecules. J. Nanosci. Nanotechnol 2006;6:2591–2607. [PubMed: 17048469]
58. Chew SY, Wen J, Yim EK, Leong KW. Sustained release of proteins from electrospun biodegradable fibers. Biomacromolecules 2005;6:2017–2024. [PubMed: 16004440]
59. Chew SY, Mi R, Hoke A, Leong KW. Aligned protein-polymer composite fibers enhance nerve regeneration: A potential tissue-engineering platform. Adv. Funct. Mater 2007;17:1288–1296. [PubMed: 18618021]
60. Jiang H, Hu Y, Zhao P, Li Y, Zhu K. Modulation of protein release from biodegradable core-shell structured fibers prepared by coaxial electrospinning. J. Biomed.Mater. Res. B. Appl. Biomater 2006;79B:50–57. [PubMed: 16544305]
61. Srikar R, Yarin AL, Megaridis CM, Bazilevsky AV, Kelley E. Desorption-limited mechanism of release from polymer nanofibers. Langmuir 2008;24:965–974. [PubMed: 18076196]
62. Taylor G. Electrically Driven Jets, Proceedings of the Royal Society of London Series a-Mathematical and Physical Sciences. 1969;313:453–475.
63. Doshi J, Reneker DH. Electrospinning Process and Applications of Electrospun Fibers. Journal of Electrostatics 1995;35:151–160.
64. He, CL.; Huang, ZM.; Han, XJ. J. Biomed. Mater. Res. Electronic publication; 2008. Fabrication of drug-loaded electrospun aligned fibrous threads for suture applications.
65. Huang Z, He C, Yang A, Zhang Y, Han X, Yin J, Wu Q. Encapsulating drugs in biodegradable ultrafine fibers through co-axial electrospinning. J. Biomed. Mater. Res 2006;39:8113–8122.
66. Jiang H, Hu Y, Li Y, Zhao P, Zhu K, Chen W. A facile technique to prepare biodegradable coaxial electrospun nanofibers for controlled release of bioactive agents. J. Control. Release 2005;108:237–243. [PubMed: 16153737]
67. Zhang YZ, Wang X, Feng Y, Li J, Lim CT, Ramakrishna S. Coaxial electrospinning of (fluorescein isothiocyanate-conjugated bovine serum albumin)-encapsulated poly(epsilon-caprolactone) nanofibers for sustained release. Biomacromolecules 2006;7:1049–1057. [PubMed: 16602720]
68. Zhang YZ, Venugopal J, Huang ZM, Lim CT, Ramakrishna S. Characterization of the surface biocompatibility of the electrospun PCL-collagen nanofibers using fibroblasts. Biomacromolecules 2005;6:2583–2589. [PubMed: 16153095]
69. Kim TG, Chung HJ, Park TG. Macroporous and nanofibrous hyaluronic acid/collagen hybrid scaffold fabricated by concurrent electrospinning and deposition/leaching of salt particles. Acta Biomaterialia 2008;4:1611–1619. [PubMed: 18640884]
70. Foltran I, Foresti E, Parma B, Sabatino P, Roveri N. Novel biologically inspired collagen nanofibers reconstituted by electrospinning method. Macromol. Symp 2008;269:111–118.
71. Ji Y, Ghosh K, Shu XZ, Li B, Sokolov JC, Prestwich GD, Clark RA, Rafailovich MH. Electrospun three-dimensional hyaluronic acid nanofibrous scaffolds. Biomaterials 2006;27:3782–3792. [PubMed: 16556462]
72. Li J, He A, Zheng J, Han CC. Gelatin and gelatin-hyaluronic acid nanofibrous membranes produced by electrospinning of their aqueous solutions. Biomacromolecules 2006;7:2243–2247. [PubMed: 16827594]
73. Dang JM, Leong KW. Myogenic induction of aligned mesenchymal stem cell sheets by culture on thermally responsive electrospun nanofibers. Adv Mater Deerfield 2007;19:2775–2779. [PubMed: 18584057]
74. Desai K, Kit K, Li J, Zivanovic S. Morphological and surface properties of electrospun chitosan nanofibers. Biomacromolecules 2008;9:000–1006.
75. Chen JP, Chang GY, Chen JK. Electrospun collagen/chitosan nanofibrous membrane as wound dressing. Colloid. Surface Physicochem. Eng. Aspect 2008;313:183–188.
76. Kim GT, Lee JS, Shin JH, Ahn YC, Hwang YJ, Shin HE, Lee JK, Sung CM. Investigation of pore formation for polystyrene electrospun fiber: effect of relative humidity. Kor. J. Chem. Eng 2005;22:783–788.

77. Deitzel JM, Kleinmeyer J, Harris D, Tan NCB. The effect of processing variables on the morphology of electrospun nanofibers and textiles. Polymer 2001;1:261–272.

78. Li XH, Shao CL, Liu YC. A simple method for controllable preparation of polymer nanotubes via a single capillary electrospinning. Langmuir 2007;23:10920–10923. [PubMed: 17880254]

79. Megelski S, Stephens JS, Chase DB, Rabolt JF. Micro- and nanostructured surface morphology on electrospun polymer fibers. Macromolecules 2002;22:8456–8466.

80. Huang F, Wei Q, Wang J, Cai Y, Huang Y. Effect of temperature on structure, morphology and crystallinity of PVDF nanofibers via electrospinning. e-Polymers 2008:152.

81. Wang C, Chien HS, Hsu CH, Wang YC, Wang CT, Lu HA. Electrospinning of polyacrylonitrile solutions at elevated temperatures. Macromolecules 2007;40:7973–7983.

82. Liao IC, Chen S, Liu JB, Leong KW. Sustained Viral Gene Delivery Through Core-shell Fibers. Journal of Controlled Release. 2009In press

83. Sung K, Lee CS. Factors influencing liquid breakup in electrohydrodynamic atomization. J. Appl. Phys 2004;96:3956–3961.

84. Chen DR, Pui DYH, Kaufman SL. Electrospraying of conducting liquids for monodisperse aerosol generation in the 4 nm to 1.8 μm diameter range. J. Aerosol. Sci 1995;26:963–977.

85. Hartman RPA, Brunner DJ, Camelot DMA, Marijnissen JCM, Scarlett B. Electrohydrodynamic atomization in the cone-jet mode physical modeling of the liquid cone and jet. J. Aerosol. Sci 1999;30:823–849.

86. Kim GH, Park JH. A PMMA optical diffuser fabricated using an electrospray method. Appl. Phys. Mater. Sci. Process 2007;86:347–351.

87. Tang KQ, Gomez A. Monodisperse electrosprays of low electric conductivity liquids in the cone-jet mode. J. Colloid Interface Sci 1996;184:500–511. [PubMed: 8978553]

88. Langer G, Yamate G. Encapsulation of liquid and solid aerosol particles to form dry powders. J. Colloid Interface Sci 1969;29:450–455.

89. Wu Y, MacKay JA, McDaniel JR, Chilkoti A, Clark RL. Fabrication of elastin-like polypeptide nanoparticles for drug delivery by electrospraying. Biomacromolecules 2009;10(1):19–24. [PubMed: 19072041]

90. Xu Y, Hanna MA. Electrosprayed bovine serum albumin-loaded tripolyphosphate cross-linked chitosan capsules: Synthesis and characterization. J. Microencapsul 2007;24:143–151. [PubMed: 17454425]

91. Hwang YK, Jeong U, Cho EC. Production of uniform-sized polymer core-shell microcapsules by coaxial electrospraying. Langmuir 2008;24:2446–2451. [PubMed: 18257594]

92. Casper CL, Yamaguchi N, Kiick KL, Rabolt JF. Functionalizing electrospun fibers with biologically relevant macromolecules. Biomacromolecules 2005;6:1998–2007. [PubMed: 16004438]

93. Li C, Vepari C, Jin HJ, Kim HJ, Kaplan DL. Electrospun silk-BMP-2 scaffolds for bone tissue engineering. Biomaterials 2006;27:3115–3125. [PubMed: 16458961]

94. Luu YK, Kim K, Hsiao BS, Chu B, Hadjiargyrou M. Development of a nanostructured DNA delivery scaffold via electrospinning of PLGA and PLA-PEG block copolymers. J. Control. Release 89;2003:341–353.

95. Liang D, Luu YK, Kim K, Hsiao BS, Hadjiargyrou M, Chu B. In vitro non-viral gene delivery with nanofibrous scaffolds. Nucleic Acids Res 2005;33:e170. [PubMed: 16269820]

96. Xu Y, Skotak M, Hanna M. Electrospray encapsulation of water-soluble protein with polylactide. I. Effects of formulations and process on morphology and particle size. J. Microencapsul 2006;23:69–78. [PubMed: 16830978]

97. Xu X, Chen X, Xu X, Lu T, Wang X, Yang L, Jing X. BCNU-loaded PEG-PLLA ultrafine fibers and their in vitro antitumor activity against glioma C6 cells. J. Control. Release 2006;114:307–316. [PubMed: 16891029]

98. Xu X, Yang L, Xu X, Wang X, Chen X, Liang Q, Zeng J, Jing X. Ultrafine medicated fibers electrospun from W/O emulsions. J. Control. Release 2005;108:33–42. [PubMed: 16165243]

99. Khil MS, Cha DI, Kim HY, Kim IS, Bhattarai N. Electrospun nanofibrous polyurethane membrane as wound dressing. J. Biomed. Mater. Res. B. Appl. Biomater 2003;67b:675–679. [PubMed: 14598393]

100. Choi JS, Leong KW, Yoo HS. In vivo wound healing of diabetic ulcers using electrospun nanofibers immobilized with human epidermal growth factor (EGF). Biomaterials 2008;29:587–596. [PubMed: 17997153]

101. Bölgen N, Vargel I, Korkusuz P, Menceloğlu YZ, Pişkin E. In vivo performance of antibiotic embedded electrospun PCL membranes for prevention of abdominal adhesions. J. Biomed. Mater. Res. B. Appl. Biomater 2007;81B:530–543.

102. Kim K, Luu YK, Chang C, Fang D, Hsiao BS, Chu B, Hadjiargyrou M. Incorporation and controlled release of a hydrophilic antibiotic using poly(lactide-co-glycolide)-based electrospun nanofibrous scaffolds. J. Control. Release 2004;98:47–56. [PubMed: 15245888]

103. Huang ZM, He CL, Yang A, Zhang Y, Han XJ, Yin J, Wu Q. Encapsulating drugs in biodegradable ultrafine fibers through co-axial electrospinning. J. Biomed.Mater. Res. A 2006;77A:169–179. [PubMed: 16392131]

104. Arya N, Chakraborty S, Dube N, Katti DS. Electrospraying: a facile technique for synthesis of chitosan-based micro/nanospheres for drug delivery applications. J.Biomed. Mater. Res. B Appl. Biomater 2009;88:17–31. [PubMed: 18386845]

105. Clarke JD, Jayasinghe SN. Bio-electrosprayed multicellular zebrafish embryos are viable and develop normally. Biomed. Mater 2008;3011001

106. Yeo LY, Gagnon Z, Chang HC. AC electrospray biomaterials synthesis. Biomaterials 2005;26:6122–6128. [PubMed: 15893816]

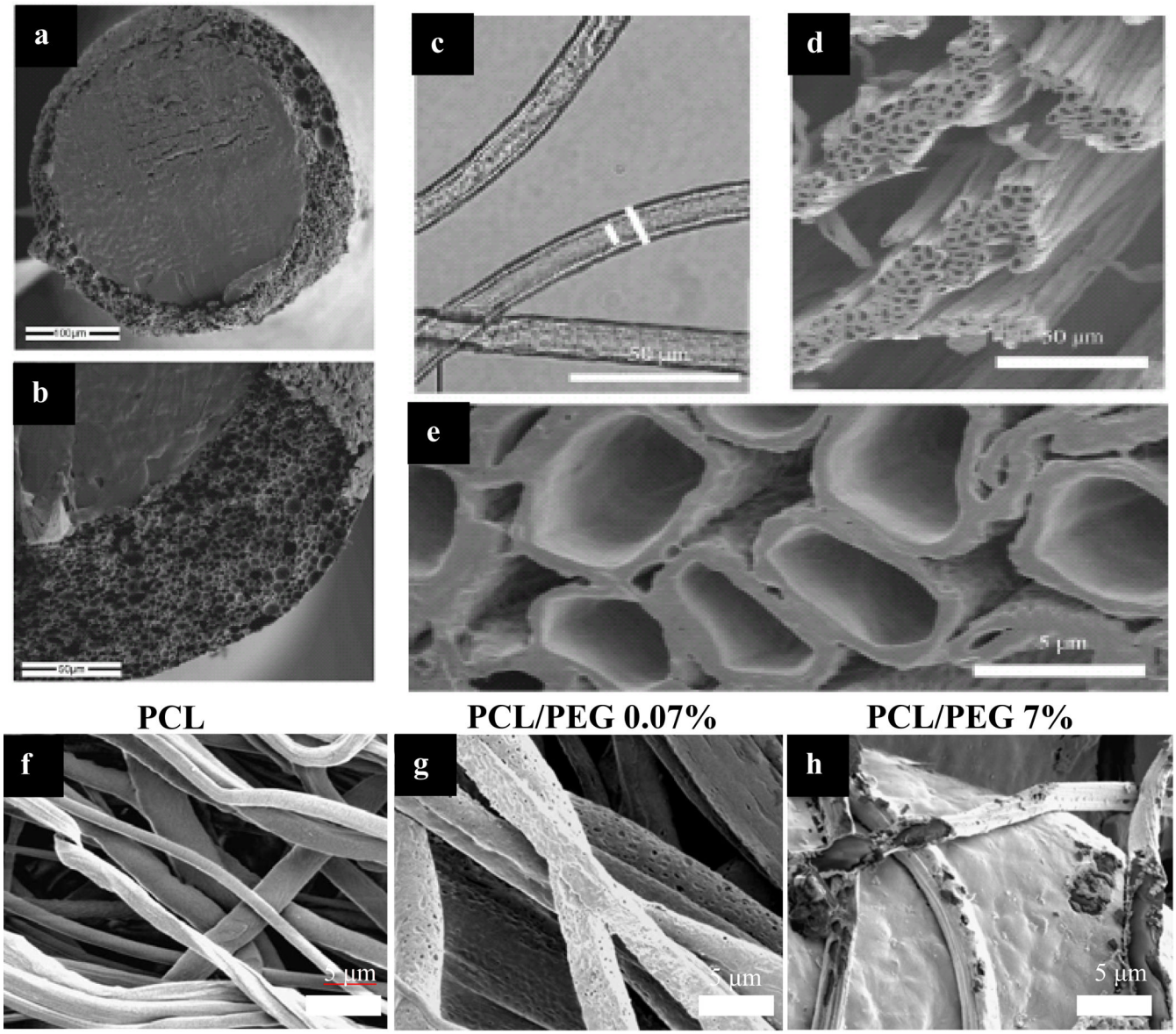

Figure 1. SEM and optical microscopy images of various morphologies of co-axial electrospun fibers

Figure 1 a and b (Top left): SEM images showing cross sections of paclitaxel-loaded core inside the PLGA shell fibers. The electrospun fibers have diameter of 200–250 μm and are designed to serve as drug eluting sutures [51] (Reprint with permission from Elsevier). Figure 1 c: Optical microscopy images of PCL hollow microtubes depicting consistent shell/core fiber size (Reprint with permission [40] from Wiley-VCH Verlag GmbH & Co. KGaA). Figure 1 d and e: SEM images of PCL hollow microtubes (Reprint with permission [40] from Wiley-VCH Verlag GmbH & Co. KGaA). Figure 1 f–h (Bottom): SEM images demonstrating the changes in surface morphology of PCL (shell) and BSA (core) fibers loaded with different concentration of PEG porogen (0%, 0.07% and 7%). At day 30, PCL fibers with no porogen (f) show no significant swelling and pore formation, while fibers with 0.07% porogen (g) have extensive development of pores on the surface. Average size of the pores is around 100 nm. Fibers with 7% porogen (h) show accelerated degradation in additional to the formed pores.

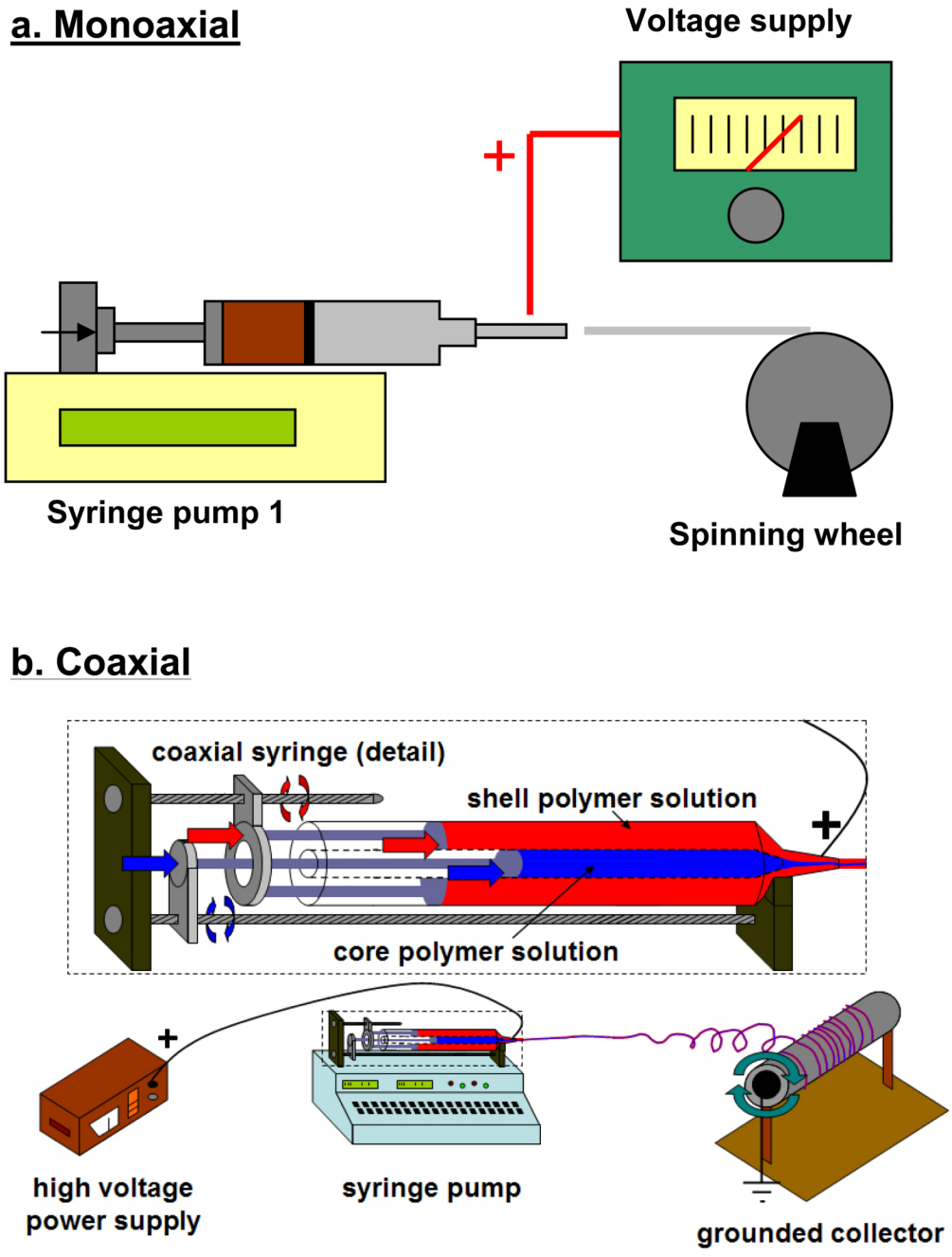

Figure 2. Various electrospinning setups used to produce mono/co-axial fibers

Figure 2a: Typical setup for mono-axial electrospinning involves the use of a syringe pump to dispense a polymer solution through a needle gauge. A high voltage gradient is applied to the needle via a power supply and the formed fibers are accelerated towards the collecting ground (spinning wheel). Figure 2b: Horizontal syringe-in-a-syringe design used in our lab for co-axial electrospinning.

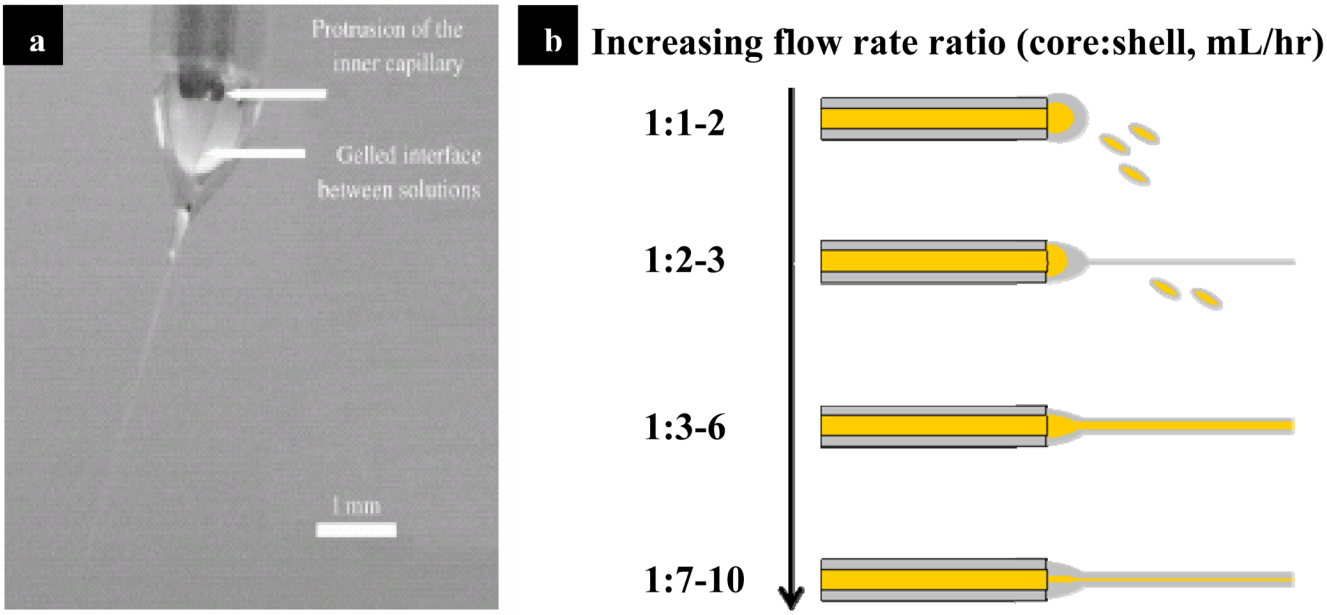

Figure 3. Co-axial electrospinning jet and its variation with alteration of flow rate ratio

Figure 3a: Image of the Taylor cone formed from the core (PEO)/shell (PCL) solution during co-axial electrospinning. (Reprint with permission [40] from Wiley-VCH Verlag GmbH & Co. KGaA). Figure 3b: An illustration of effect of different flow rate ratio in the encapsulation of core solution.

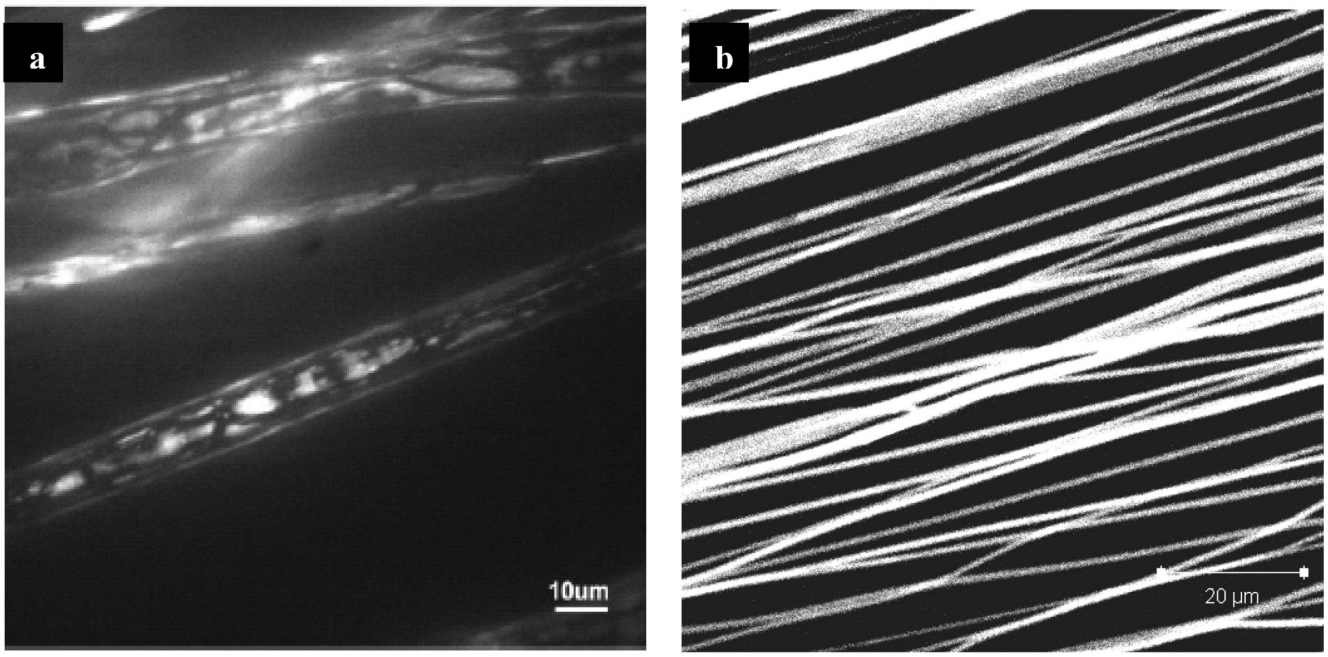

Figure 4. Distribution and uniformity of FITC-BSA encapsulated via mono-axial and co-axial electrospinning

Figure 4a: Confocal microscopy of FITC-BSA encapsulated into electrospun PCL fibers by dispersing albumin in the polymer solution. (Reprint with permission [58] from American Chemical Society). Figure 4b: Confocal microscopy of PCL (shell) fibers encapsulating FITC-BSA (core) via co-axial electrospinning.

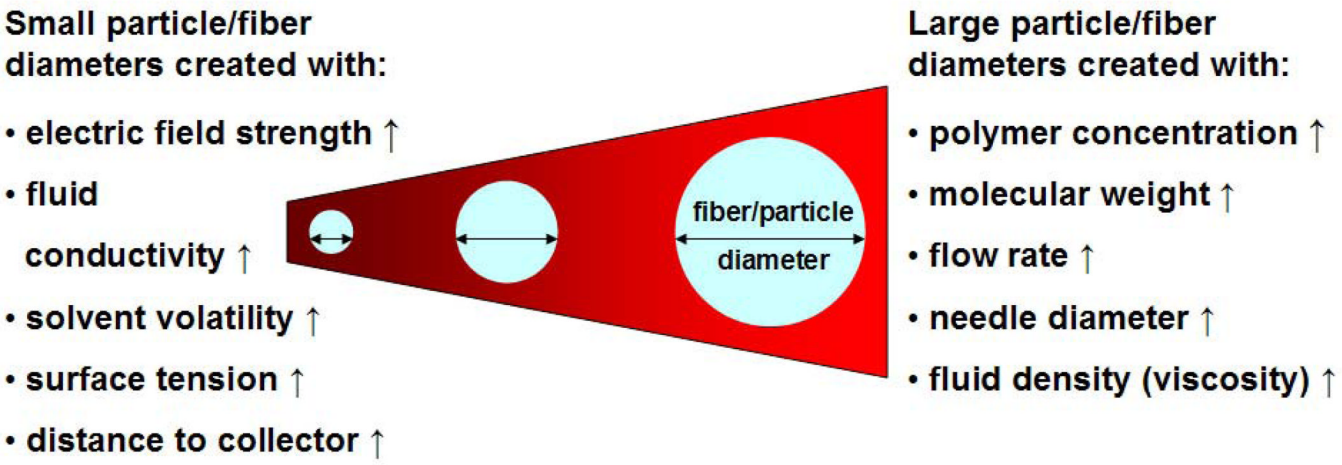

Figure 5. Diagram depicting the influence of electrospinning/spraying parameters on the diameter of fiber/particle
(↑: Increase).

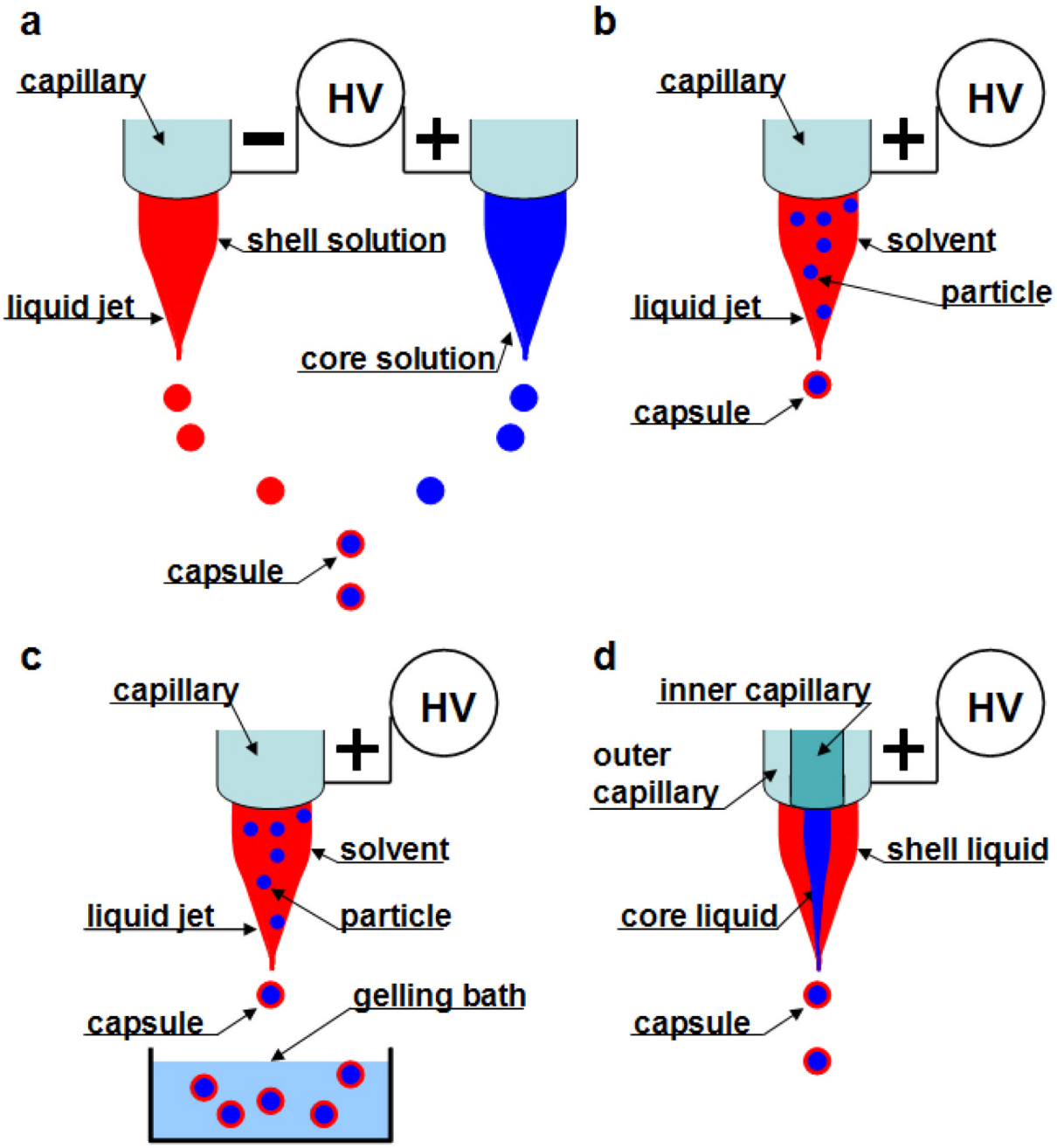

Figure 6. Schematics of various electro-encapsulation processes (Adapted from [25] with permission from Elsevier)

(a) Collision of droplets of opposite polarity; (b) Electrospraying of a drug dissolved/suspended in polymer with solidification by evaporation; (c) Electrospraying of a drug dissolved/ suspended in polymer with solidification by a chemical or ionic crosslinker; and (d) Coaxial Electrospraying.

Table 1

Effect of alteration of electrospinning parameters on the release rate of various drugs in different polymer systems.

Parameter	Drug of interest	Polymer carrier	Effect	Reference
Polymer MW ↑	Rhodamine 610	PCL	Release rate ↓	[72]
		PMMA		
Polymer concentration ↑	Rhodamine 610	PCL	Release rate ↓	[72]
		PMMA		
	Paclitaxel	PLGA		[53]
	Tetracycline hydrochloride	PLLA		[45]
Core - drug interaction ↑	Rhodamine 610	PCL	Release rate ↓	[72]
Polymer degradability ↑	Rhodamine 610	PCL	Release rate ↑	[72]
		PMMA		
	Paclitaxel	PLGA		[62]
		PMMA		
Drug concentration ↑	Paclitaxel	PLGA	Release rate ↑	[53]
Porogen concentration↑	BSA	PCL	Release rate ↑	[55] [78] [71]
	PDGF-bb			[55]
Porogen MW ↑	BSA	PCL	Release rate ↓	[55]
Porosity ↑	Paclitaxel	PLGA	Release rate ↑	[53]
Flow rate ratio (S:C) ↑	BSA	PCL	Release rate ↓	[71]